# A MESOSCALE SIMULATION STUDY OF A HEAVY RAIN EVENT OVER SOUTHERN TAIWAN IN MEIYU SEASON

**Lisa T. C. Chang[1,2] George T. J. Chen[1]**

**[1]Department of Atmospheric Sciences, National Taiwan University, Taiwan**

**[2]Department of Environmental Engineering, Tung Nan Institute of Technology, Taiwan**

## 1. Introduction

There are about 4-5 frontal systems affecting Taiwan during Meiyu season each year (Chen 1988). The Meiyu front is usually accompanied by a nearly continuous cloud band, which produces stratiform and/or convective precipitation (Chen 1992). During the period of 29-30 May 2001, a series of mesoscale convective systems (MCSs) developed in the vicinity of Taiwan along a retrograde moving Meiyu front. The development and northeastward propagation of the MCSs produced heavy rainfall over southern Taiwan, with a maximum 24-h accumulation rainfall of 200 mm. This study concentrates on the most intense precipitation that occurred during 12 UTC 29 May to 00 UTC 30 May. To further understand the physical process related to the heavy rain event, the atmospheric component of the Naval Research Laboratory's (NRL) Coupled Ocean/Atmosphere Mesoscale Prediction System (COAMPS; Hodur 1997) is performed in this study. In order to include mesoscale features in the model initial condition, satellite scatterometer QuikSCAT surface wind measurements (Graf et al. 1998) are blended into the COAMPS analysis procedure where the NOGAPS global analysis data were used as the first guess. The successful simulation also provides further insight and understanding into the moisture transport processes related to convective precipitation.

## 2. Model description and design of experiment

COAMPS is a nested, three-dimensional model that solves the non-hydrostatic, fully compressible equations of motion on terrain-following sigma coordinate $\sigma_z$. Horizontal grid increment of 45, 15 and 5 km are used for the coarse, medium and fine-mesh grids, respectively (Fig. 1). There

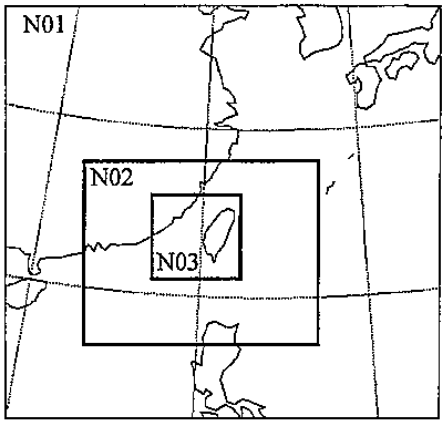


Fig.1. Domain configuration (N01, N02, N03) for COAMPS model simulation.

are 30 layers in the vertical, 12 of which are below 1.5 km for higher vertical resolution in the boundary layer. Assimilation cycles with 12-h periods starting from 1200 UTC 28 May (hereafter 052812) to 053012 are performed in COAMPS (Fig. 2). The cycles begin with a cold start (CS) that refers to a COAMPS simulation that is initialized directly from the NOGAPS analyses, while the later warm starts (WS) refer to a COAMPS run that is restarted from a previous 12-h forecast. Throughout the simulation, NOGAPS forecast fields are adopted as the lateral boundary conditions.

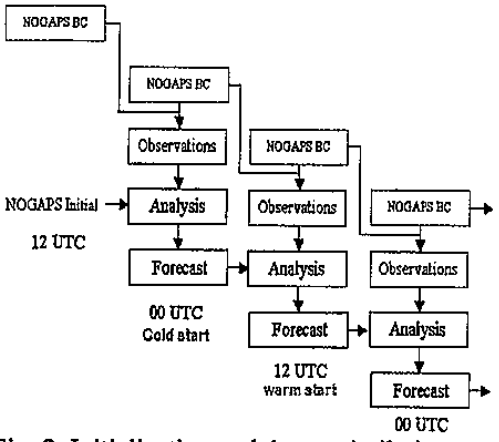


Fig. 2. Initialization and data assimilation cycle of COAMPS.

Two experiments, namely, the control (CTNL) and QuikSCAT (QUIK), are performed. Both simulations have the same full physics, except the QUIK experiment is conducted by blending QuikSCAT oceanic surface wind in 50-km resolution using the Multivariate Optimum Interpolation (MVOI) scheme (Barker 1992) into the initial conditions of every 12-h assimilation cycle.

## 3. Case description and model validation

GMS-5 satellite imagery indicates the MCS A first developed and enhanced over southern Taiwan around 15-18 UTC 29 May along the Meiyu frontal cloud band (Fig. 3).

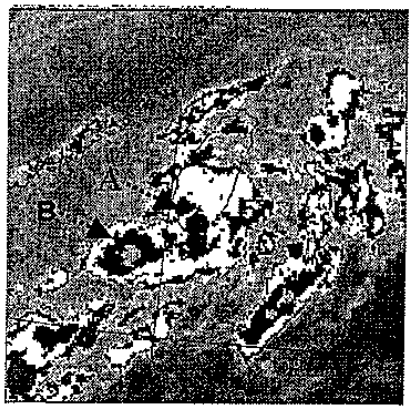


Fig. 3. GMS infrared image for 18 UTC 29 May

About the same time, MCS B initiated over southern Taiwan Strait and propagated downstream toward southern Taiwan in the subsequent hours. The 6-h accumulated precipitation mainly produced by MCS A was larger than 50 mm (Fig. 4). Localized rainfall maximums are found near the central coastal plain and over the southern tip of Taiwan

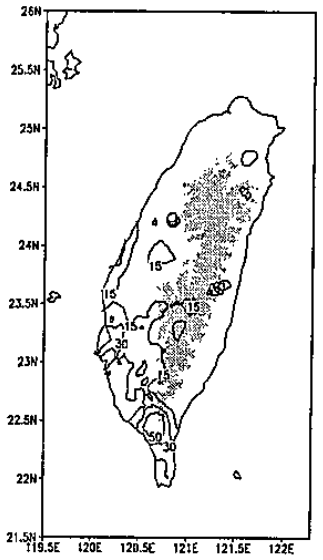


Fig. 4 CWB observed 6-h accumulated precipitation (contour levels of 15, 30 and 50mm) at 18 UTC 29 May 2001. Model terrain height above 1500 m is shaded.

The closest time to the simulation period with available TRMM rainfall estimations (Kummerow 2000) is at 00 UTC 30 May 2001 (Fig 5a). There were maximum precipitation areas over the ocean to the northeast as well as to the southwest of Taiwan. COAMPS simulated precipitation in the 45-km grid from CTNL experiment valid at 00 UTC 30 May has a smaller amount of precipitation over both the southern Taiwan Strait and over the ocean northeast to Taiwan (Fig. 5b). On the other hand, the QUIK experiment generates better simulated precipitation in terms of both the amount and the spatial distribution (Fig. 5c).

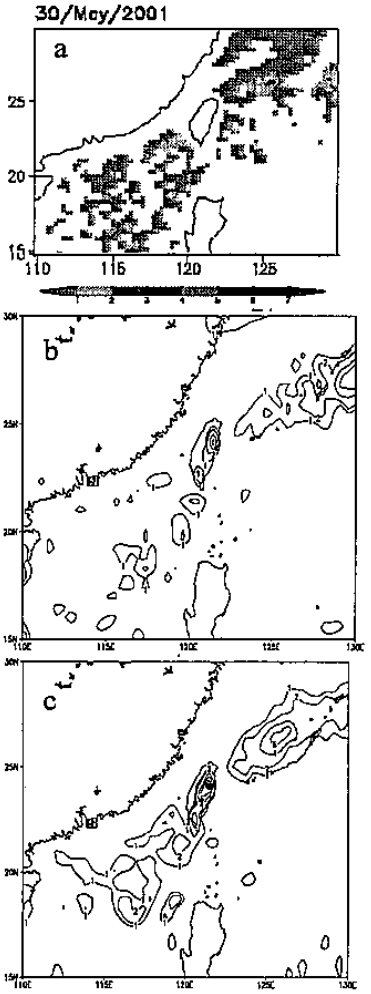


Fig. 5. (a) TRMM observed rainfall rate at 00 UTC 30 May 2001 (shading, in mm) (b) simulated precipitation in 45-km grid of CTNL (contour levels of 1, 2, 4 and 6 mm) valid at 00 UTC 30 May 2001 ( c ) as in (b), except of QUIK.

As in Yeh et al. (2002), kinematic characteristics of the Meiyu front in the 15-km model gird of both the CTNL and QUIK experiments are further examined in order to study the impact of better resolved surface winds. At 12 UTC 29 May, the surface wind shift line in CTNL experiment shows a light shift to the north (Fig. 6b) compared to that in QuikSCAT (Fig. 6a), whereas the corresponding areas from the QUIK experiment are closer to the wind shift line (Fig. 6c). In addition, the simulated area of maximum cyclonic vorticity at the western portion of wind shift line from QUIK experiment (Fig. 6c) is closer to that derived from QuikSCAT in Fig. 6a.

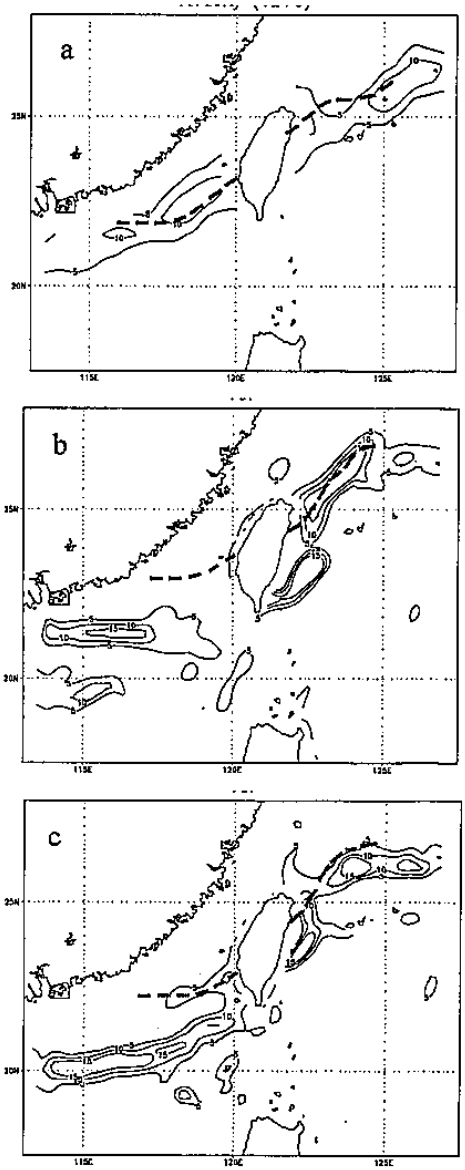


Fig. 6. (a) QuikSCAT-derived relative vorticity at 12 UTC 29 May 2001 (b) the CTNL simulation in 15-km grid domain valid at 12 UTC 29 May 2001 at 1000 hPa for relative vorticity, (c) as in (b), except for QUIK simulation. Dash lines indicate frontal wind shift line. Contours are analyzed at $5\times10^{-5}$ $s^{-1}$

Simulated 3-h accumulated precipitation in the 5-km grid from both experiments is also studied. During the period of 12-18 UTC 29 May, the CTNL experiment does not reproduce the precipitation to the south of

Taiwan well (not shown). Comparatively, the precipitation pattern is much better reproduced by the QUIK. There are two areas of local maximum in Taiwan in the three-hour accumulated rainfall valid at 15 UTC and 18 UTC 29 May (Fig 7), which is quite similar to the observed rainfall pattern (Fig. 4). Furthermore, the QUIK experiment also reproduces the precipitation successfully over the southern Taiwan Strait brought largely by MCS B. Since the QUIK experiment reproduces the overall rainfall distribution satisfactorily. It allows detailed calculations of the mesoscale moisture budget, in particular, in the boundary layer that are essential to understanding the origin of moisture associated with the convection initiated over the ocean (i.e. MCS B in this study) The computation methodology and preliminary results are described in section 4.

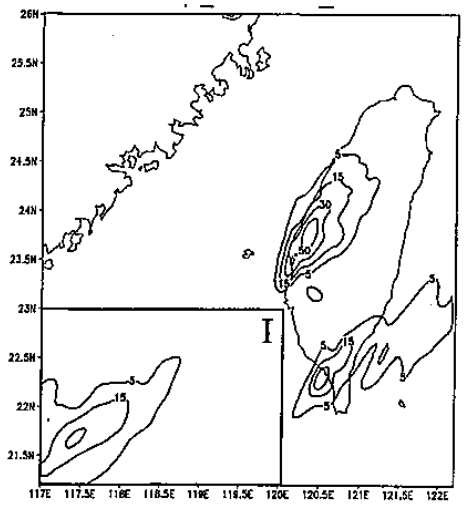


Fig. 7 Simulated 3-h accumulated precipitation in the 5-km grid of QUIK at 18 UTC 29 May. The subdomain I is for calculating area-average moisture budget in section 4.

## 4. Diagnose of Moisture budget

The moisture budget equation in height coordinate with the molecular diffusion term neglected and portioned the variables into mean (bar) and turbulent (prime) part, can be written as,

$$\underbrace{\frac{\partial \bar{q}}{\partial t}}_{A}+\underbrace{\nabla\cdot\overline{\vec{V}q}}_{B}+\underbrace{\frac{\partial \overline{wq}}{\partial z}}_{C}=\underbrace{-(\nabla\cdot\overline{\vec{V}'q'}}_{D}+\underbrace{\frac{\partial(\overline{w'q'})}{\partial z}}_{E})+\underbrace{\frac{S}{\rho}}_{F}$$

where q is specific humidity of water vapor, V horizontal wind vector, w vertical velocity in height coordinate, $\rho$ air density, and S sources and sinks of water vapor. Term A represents the local time change of mean total moisture, while term B and C denotes mean total horizontal and vertical moisture flux divergence, respectively. The mean quantities in terms A, B and C are calculated from results in the 5-km resolution grid. On the RHS of equation, the sets of prime terms in terms D and E represents the divergence of turbulent moisture flux, which is calculated implicitly by employing K-theory of the 5-km resolution grid. The last term F is the source/sink term. It is computed as a residual term to balance the other terms. A simple centered finite-difference scheme is used to compute all spatial and time derivates.

Budget calculation is employed prior to and during the convective outbreak in the subdomain I (Fig. 7) during the period of 13 UTC to 23 UTC 29 May 2002, while MCS B within domain was related to a frontal convection translated from outside the southwestern corner of the domain as well as local development. The values then averaged over grids where precipitation occurred that are defined as moisture variation related to convective activity. On the other hand, values averaged over grids where precipitation is absent represent the processes related with water vapor fluctuations in the environment.

In order to investigate moisture varying content in the environment through both grid and subgrid scale processes in the boundary layer, non-precipitation area average budget values in height-time cross sections for the surface-1100 m layer are given in Fig. 8. In Fig. 8a, the strong horizontal moisture convergence in the environment occurs below 200 m during the entire analyzed period. The strong horizontal moisture convergence may lead to the increase of local water vapor content that is carried up by the vertical moisture flux divergence in the boundary layer (not show). The positive value appears in Fig. 8b implies the occurrence of the vertical turbulent moisture flux divergence, which is and order of magnitude larger than horizontal turbulent moisture flux convergence (not shown). It leads to a significant upward turbulent moisture transport in the layer below 1100 m. Positive values in Fig. 8c implies water vapor accumulated from unresolvable processes such as evaporation, which may lead to the moistening of the boundary layer. It should be noted that the intensive gradient of residual and turbulent vertical moisture flux divergence below 50 m illustrates moisture accumulated through intense evaporation over the ocean surface may be transported

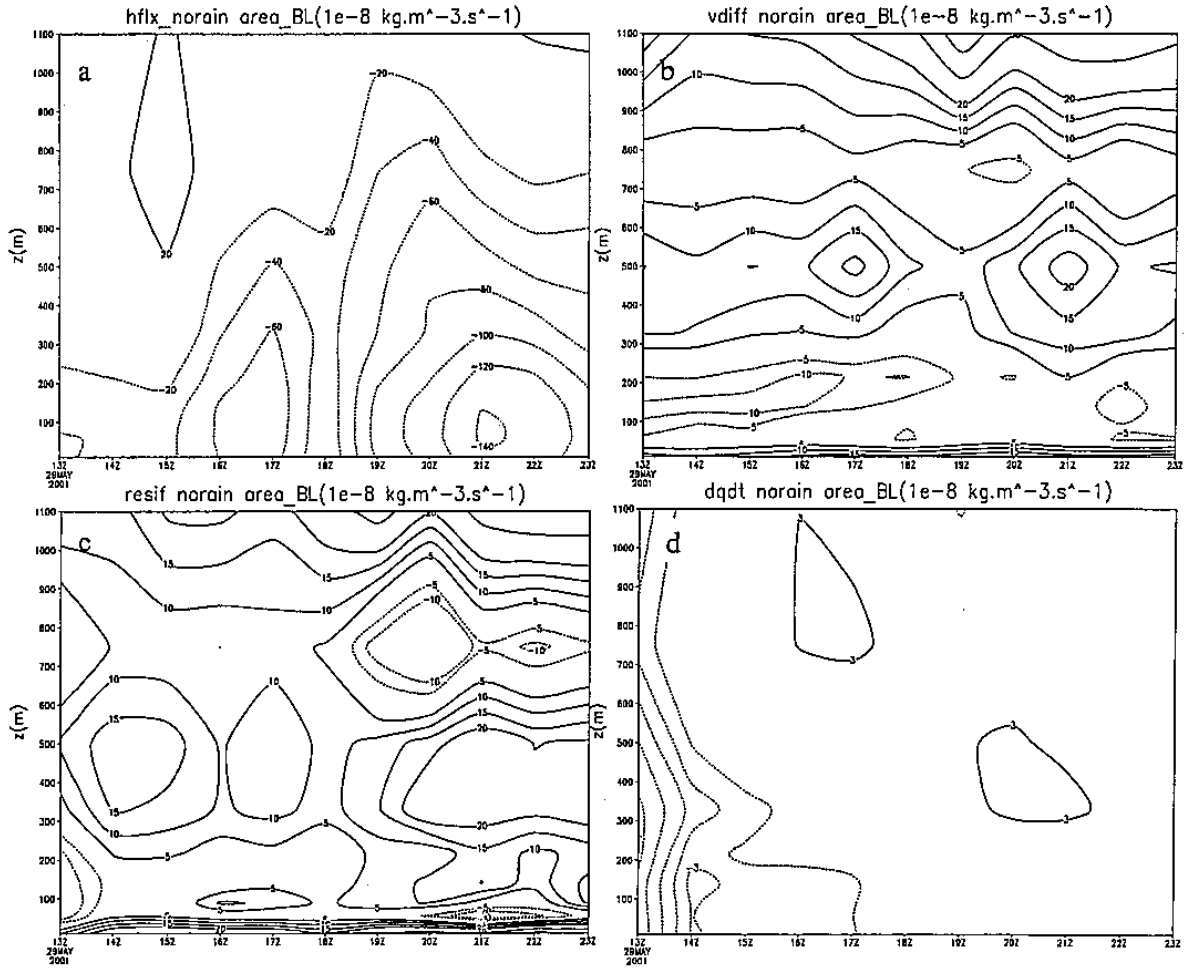


Fig.8 Height-Time cross sections of non-precipitation area averaged moisture budget terms ($10^{-8}$ kg $m^{-3}$ $s^{-1}$) from 13 UTC to 23 UTC 29 May 2001 in the layer of surface-1100 m for (a) horizontal flux divergence, (b) vertical turbulent flux divergence, (c) residual and (d) local water vapor change

upward into upper layer by sub-grid scale turbulent process. The grid-scale vertical transport is comparably less important in the very low boundary layer.

Although the intense grid scale and sub-grid scale moisture transport into subdomain 1 in the boundary layer, the water vapor content has relatively slight change (Fig. 8d). The net effect of resolvable grid scale moisture transport is to carry the water vapor upward into the middle troposphere. In addition, subgrid grid scale turbulent mixing is crucial in transporting the water vapor accumulated by evaporation from the ocean surface upward in to higher level of boundary layer.

## 5. Summary

The COAMPS simulations were conducted with full physics to evaluate the ability of the model to reproduce the evolution of MCSs and heavy rainfall event over southern Taiwan. To sum up, blending QuikSCAT surface winds into model assimilation cycles did improve the forecast significantly. Comparison of the model simulations, the QUIK experiment has a better agreement with all the surface features associated with Meiyu front and reproduces the overall rainfall distribution satisfactorily. The successful simulation allows detailed calculations of the mesoscale moisture budget, in particular, in the boundary layer that are essential to understanding the origin of the convection initiated over the ocean.

The preliminary results from moisture budgets diagnoses indicate the environment is characterized by strong horizontal moisture flux convergence. The net effect of resolvable grid scale moisture transport is the vertical motion carrying the moisture upward away from boundary layer and into middle troposphere. Intense evaporation in the lower boundary layer occurs over the entire analyzed period. Divergence of vertical turbulent moisture flux seems to play a significant role in carrying moisture accumulated from evaporation near ocean surface upward into higher level of boundary layer.

*Acknowledgments.* This study was supported by National Science Council of ROC under Grants NSC92-2111-M-002-006.

### References

Chen, G.T.J., 1988: On the synoptic-climatological characteristics of the east Asian Mei-Yu front. *Atmos. Sci., 16,* 435-446 (in Chinese with English abstract).

Chen, G.T.J., 1992: Mesoscale features observed in the Taiwan Mei-Yu season. *J. Meteor. Soc. Japan, 70,* 435-446.

Graf, J., C. Sasaki, C. Winn, W. T. Liu, W. Tsai, M. Freilich, and D. Long, 1998: NASA Scatterometer Experiment. Asta Astronaut., 43, 397-407.

Hodur, R.M., 1997: The Naval Research Laboratory's Coupled Ocean/Atmosphere Mesoscale Prediction System (COAMPS). *Mon. Wea. Rev.*, **125**, 1414-1430.

Kummerow, C., and Coauthors, 2000: The status of the Tropical Rainfall Measuring Mission (TRMM) after two years in orbit. *J. Appl. Meteor.*, **39**, 1965–1982.

Yeh, H. C., G. T. J. Chen, and W. T. Lin, 2002: Kinematic Characteristics of a Mei-yu Front Detected by the QuikSCAT Oceanic Winds. *Mon. Wea. Rev.*, **130**, 700–711.